Supplementary Information

Phosphorylated Cellulose Nanofiber Membranes with High Proton Conductivity for Polymer Electrolyte Membranes

Yoshimasa Matsuo [a], Taisei Kimura [a], Hinako Koyanagi [a], Natsuki Netsu [a], Fuwa Komatsu [a], Takashi Nagata [b], Shotaro Nishitsuji [c], Jun Matsui [d] and Akito Masuhara* [a, e]

a Graduate School of Science and Engineering, Yamagata University, 4-3-16 Jonan Yonezawa, Yamagata 992-8510, Japan

b Faculty of Engineering, Yamagata University, 4-3-16 Jonan Yonezawa, Yamagata 992-8510, Japan

c Graduate School of Organic Materials Science, Yamagata University, 4-3-16 Jonan, Yonezawa, Yamagata 992-8510, Japan

d Faculty of Science, Yamagata University, 1-4-12 Kojirakawa-machi, Yamagata 990-8560, Japan

e Frontier Center for Organic Materials, Yamagata University, 4-3-16 Jonan Yonezawa, Yamagata 992-8510, Japan

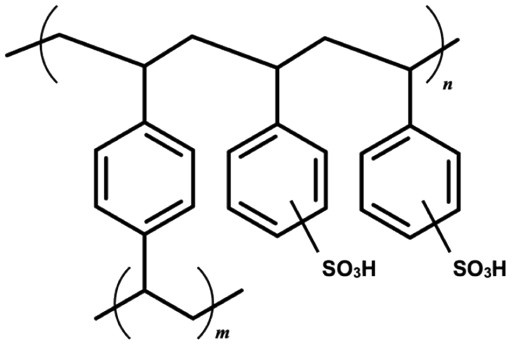

Figure S1. Chemical structure of DIAION™

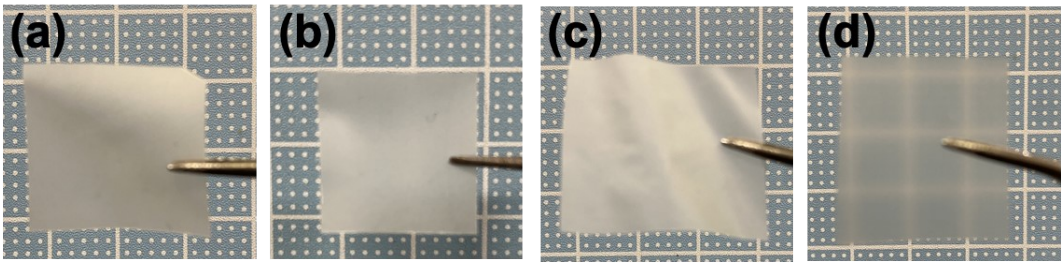

Figure S2. The images of (a) CNF, (b) P-CNF-1 h, (c) P-CNF-1.5 h and (d) P-CNF-2 h membrane.

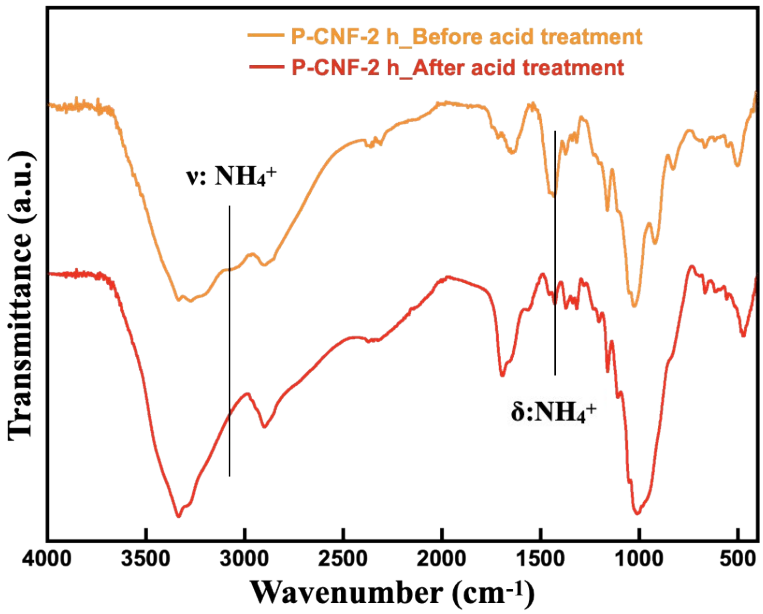

Figure S3. FTIR spectra of P-CNF-2 h membranes before acid treatment (orange line) and after acid treatment (red line).

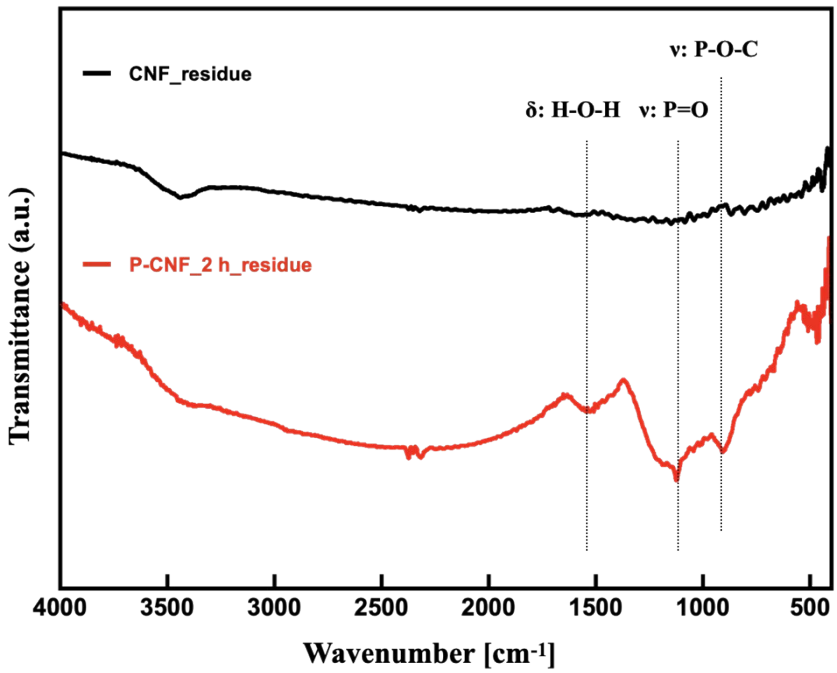

Figure S4. FT-IR (KBr method) spectra of CNF and P-CNF-2h residues after TGA measurement at 600°C under N_2 atmosphere.

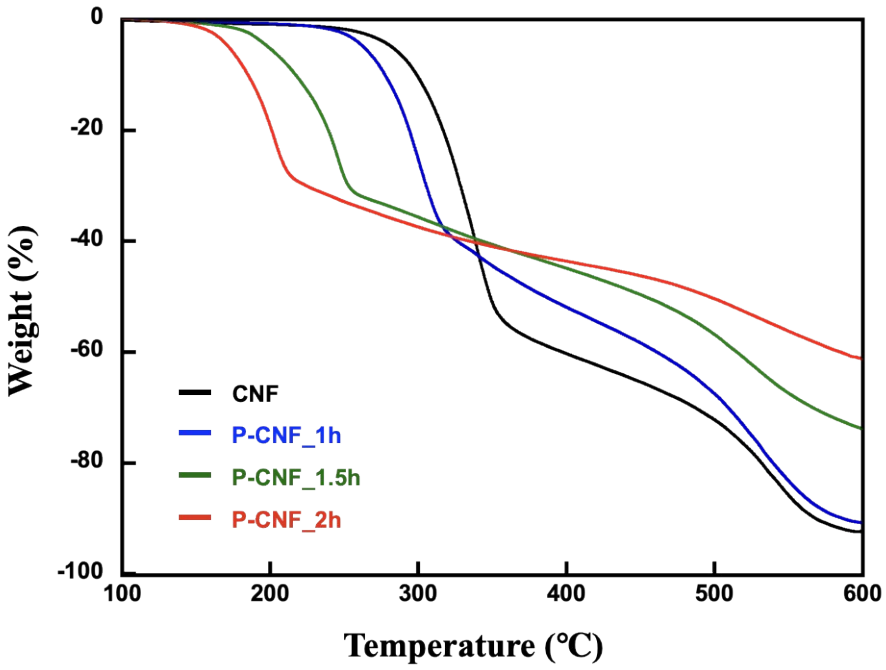

Figure S5. TGA curve measured under an air atmosphere of CNF and each P-CNF.

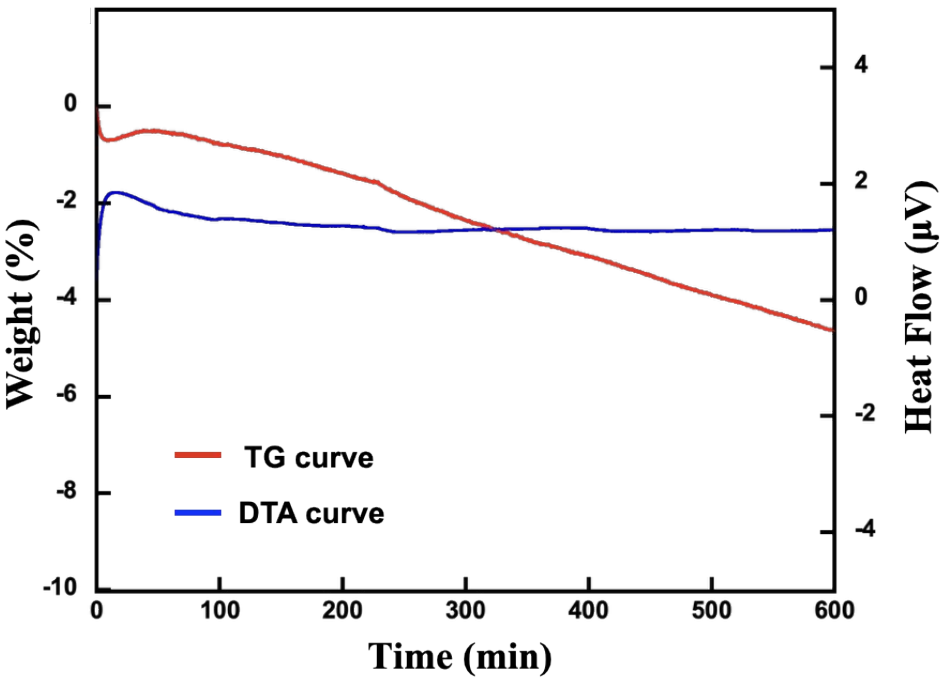

Figure S6. Isothermal TGA/ DTA curve measured under a N_2 atmosphere of P-CNF-2h.

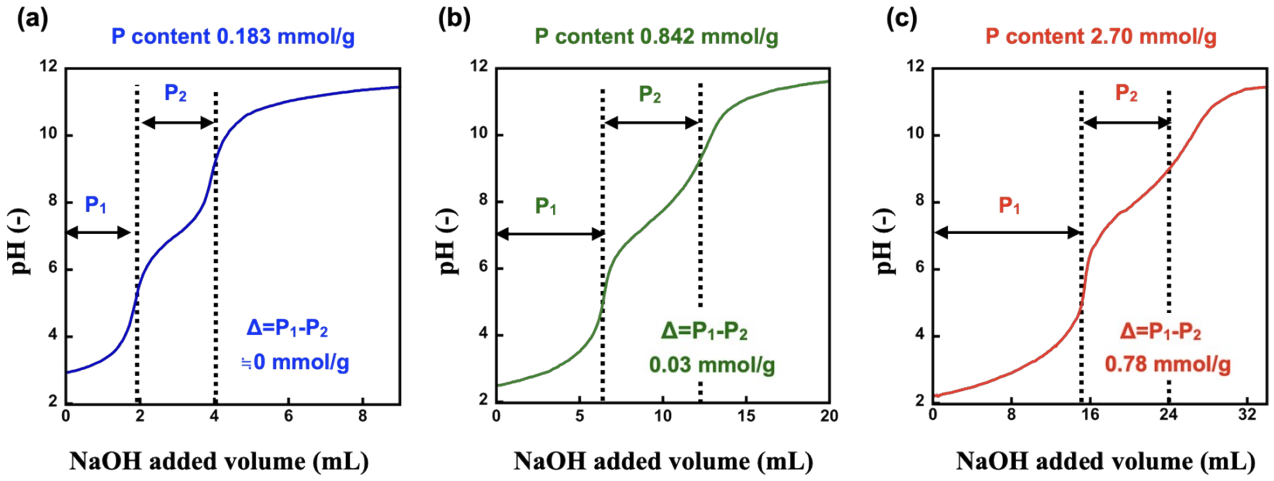

Figure S7. Titration curve of (a) P-CNF-1 h, (b) P-CNF-1.5 h, and (c) P-CNF-2 h. P_1 and P_2 are the volume of NaOH solution for the neutralization of the strong and weak acid of phosphorous groups, respectively.

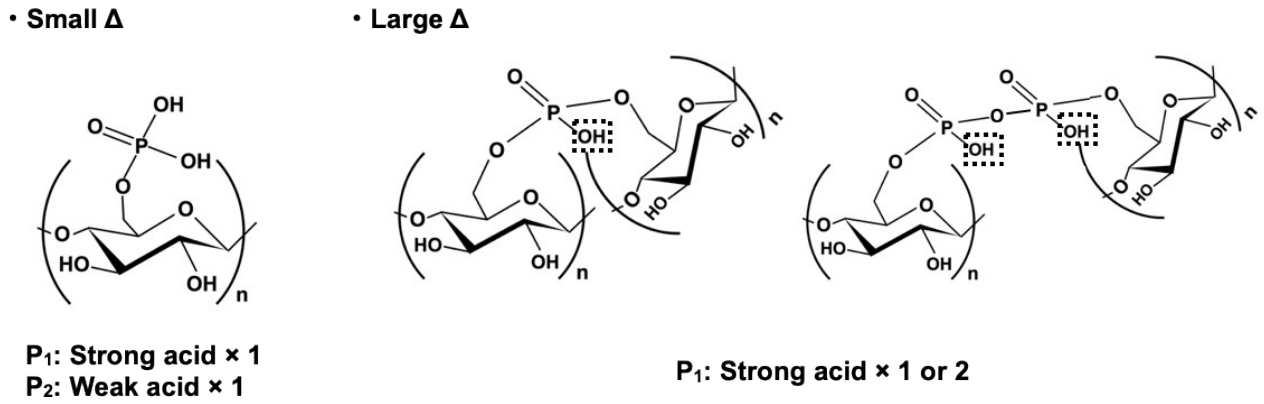

Figure S8. The structure of phosphorylated cellulose predictable from Δ.

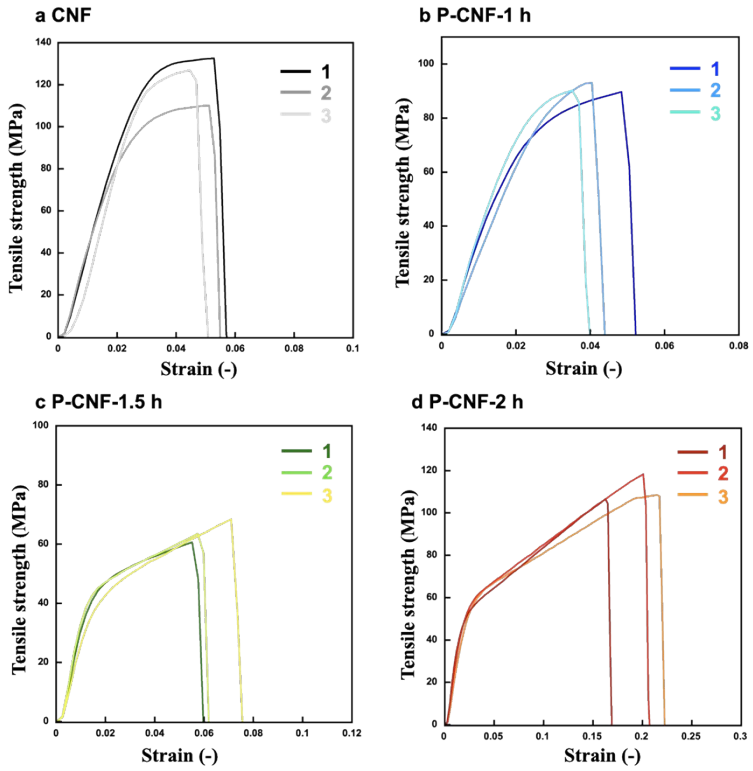

Figure S9. Stress-strain curves of the (a) CNF, (b) P-CNF-1 h, (c) P-CNF-1.5 h, and P-CNF-2 h membranes by 3 times tensile test.

Table S1. Summary of average tensile strength and strain at break of the CNF and P-CNF membranes.

membranes	Stress at break (MPa)	Strain at break (-)
CNF	123.1 (±8.0)	0.0495 (±0.0067)
P-CNF-1 h	91.0 (±1.5)	0.0413 (±0.0054)
P-CNF-1.5 h	64.2 (±3.2)	0.0612 (±0.0070)
P-CNF-2 h	111.1 (±5.2)	0.193 (±0.022)

Oxygen permeability test

Oxygen permeability tests of the Nafion and P-CNF-2 h membrane were measured on GTR-10XASS gas barrier testing system (GTR Tec corp., Japan). To measure the gas permeability, the test gas pressure was set at 101.3 kPa. The temperature for the measurement was 40 °C without humidity control. The volume of the permeated gas was measured via gas chromatography (TCD, G2700, Yanaco, Japan). The gas permeability was measured using the following equation, (O_2 permeability) ($cm^3/(m^2$ 24h atm)) = $q \times k' / (a \times t \times \Delta P)$, where q is the permeated volume of gas, k' is the correction coefficient , a is the area of the sample (15.2 cm^2), t is the measurement time and ΔP is the pressure difference (1 atm=101.3 kPa).

Table S2. Oxygen permeability measurement at 40℃ without humidity control under atomospere.

Membranes	Oxygen permeability ($cm^3/(m^2$ · 24h · atm))
Nafion 212	3.00×10^3
P-CNF-2 h membrane	2.19

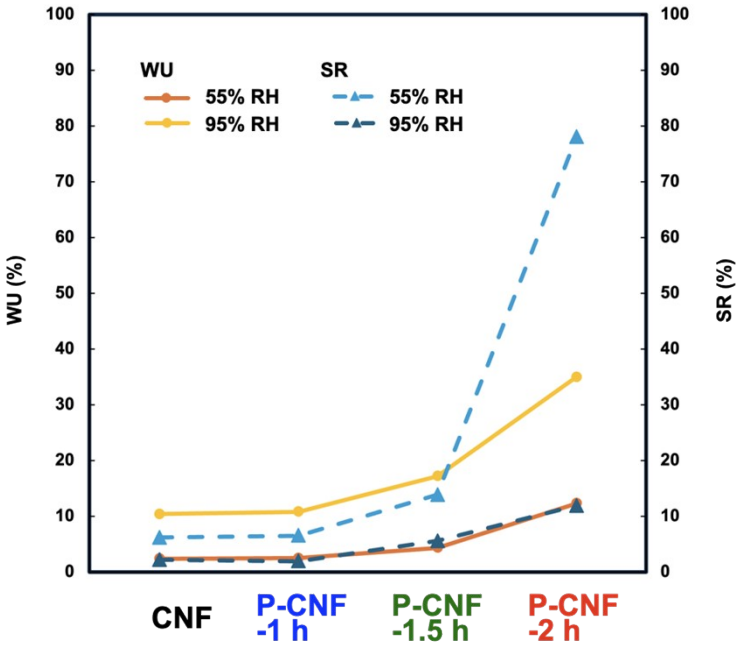

Figure S10. Water uptake and swelling ratio of CNF membranes at 80°C under 55% RH and 95% RH.

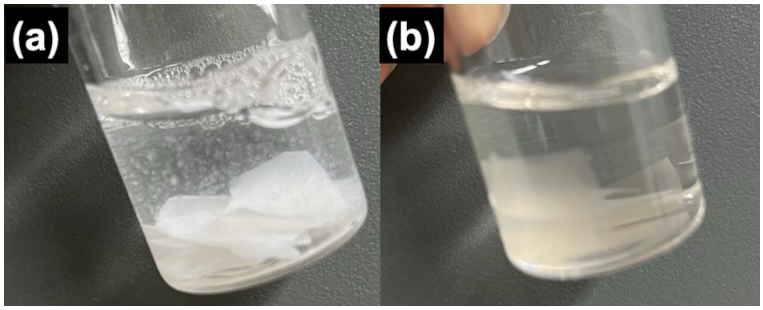

Figure S11. Images after ultrasonic treatment of the (a)CNF and (b)P-CNF-2h membranes in water.

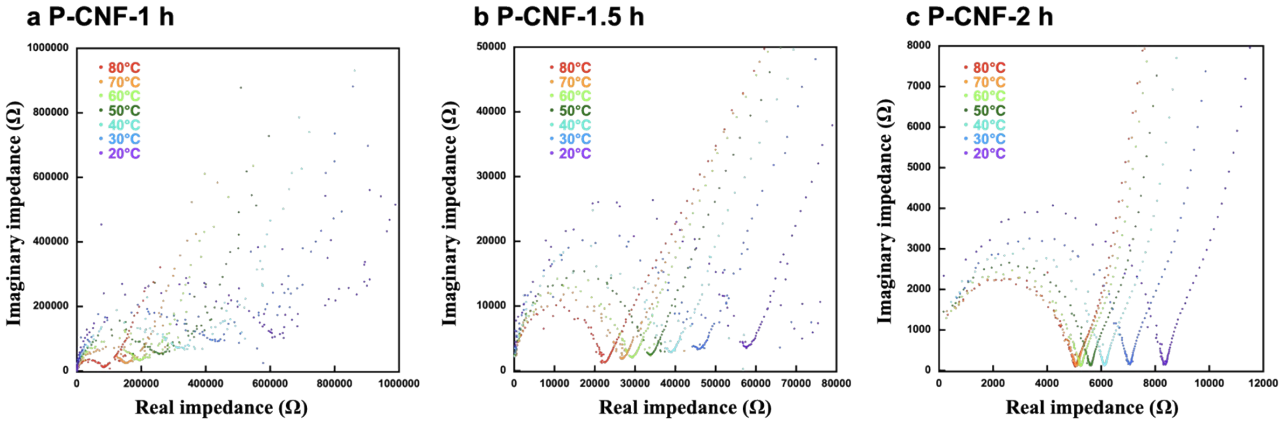

Figure S12. Cole-Cole plots of (a) P-CNF-1 h, (b) P-CNF-1.5 h, and (c) P-CNF-2 h membranes at 95% RH.

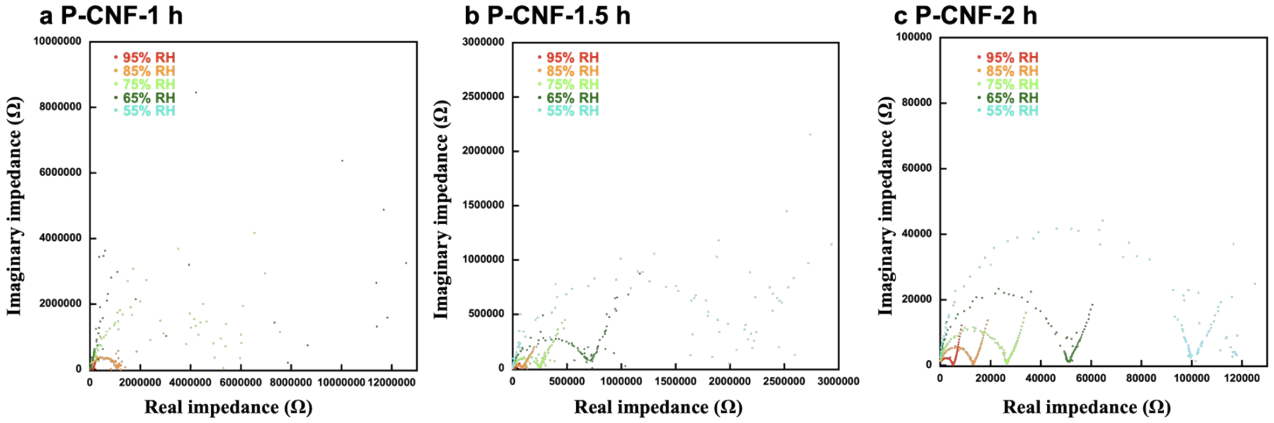

Figure S13. Cole-Cole plots of (a) P-CNF-1 h, (b) P-CNF-1.5 h, and (c) P-CNF-2 h membranes at 80°C.

Table S3. Summary of the proton conductivities of Nafion 212, CNF, and each P-CNF membrane at different temperatures at 95% RH.

Sample	Proton conductivity under 95% RH (S/cm)						
	80°C	70°C	60°C	50°C	40°C	30°C	20°C
Nafion 212	2.1×10^{-1}	1.8×10^{-1}	1.6×10^{-1}	1.3×10^{-1}	1.1×10^{-1}	8.6×10^{-2}	6.6×10^{-2}
CNF	3.9×10^{-5}	3.0×10^{-5}	2.1×10^{-5}	2.0×10^{-5}	1.0×10^{-5}	5.1×10^{-6}	1.9×10^{-6}
P-CNF-1 h	2.6×10^{-3}	1.4×10^{-3}	1.1×10^{-3}	8.3×10^{-4}	6.8×10^{-4}	5.1×10^{-4}	3.5×10^{-4}
P-CNF-1.5 h	1.4×10^{-2}	1.1×10^{-2}	1.0×10^{-2}	8.7×10^{-3}	7.7×10^{-3}	6.5×10^{-3}	5.1×10^{-3}
P-CNF-2 h	1.2×10^{-1}	1.2×10^{-1}	1.1×10^{-1}	1.1×10^{-1}	9.7×10^{-2}	8.4×10^{-2}	7.1×10^{-2}

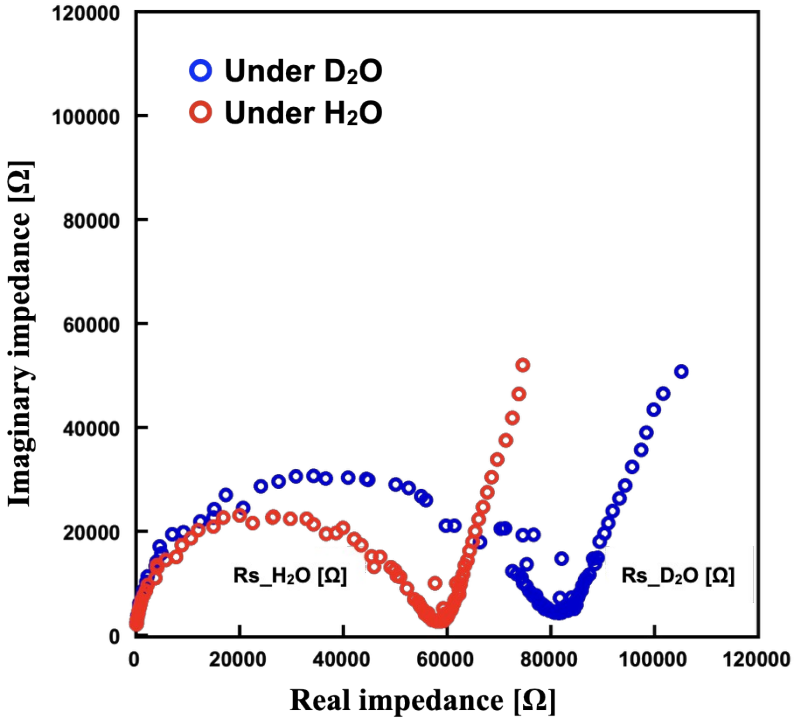

Figure S14. Cole-Cole plots of P-CNF-2 h membrane measured at 60°C under H_2O (red circle) or D_2O (blue circle) (80–85% RH) atmospheres.

Table S4. Summary of proton conductivities of Nafion 212, CNF, and each P-CNF membrane at different relative humidities (RHs) at 80°C.

Sample	Proton conductivity at 80°C (S/cm)				
	95% RH	85% RH	75% RH	65% RH	55% RH
Nafion 212	2.1×10^{-1}	1.4×10^{-1}	1.0×10^{-1}	7.3×10^{-2}	5.1×10^{-2}
CNF	3.9×10^{-5}	1.2×10^{-5}	3.0×10^{-6}	7.6×10^{-7}	2.1×10^{-7}
P-CNF-1 h	2.6×10^{-3}	2.8×10^{-4}	5.6×10^{-5}	2.3×10^{-5}	-
P-CNF-1.5 h	1.4×10^{-2}	3.6×10^{-3}	1.2×10^{-3}	4.2×10^{-4}	1.4×10^{-4}
P-CNF-2 h	1.2×10^{-1}	4.6×10^{-2}	2.2×10^{-2}	1.2×10^{-2}	6.0×10^{-3}

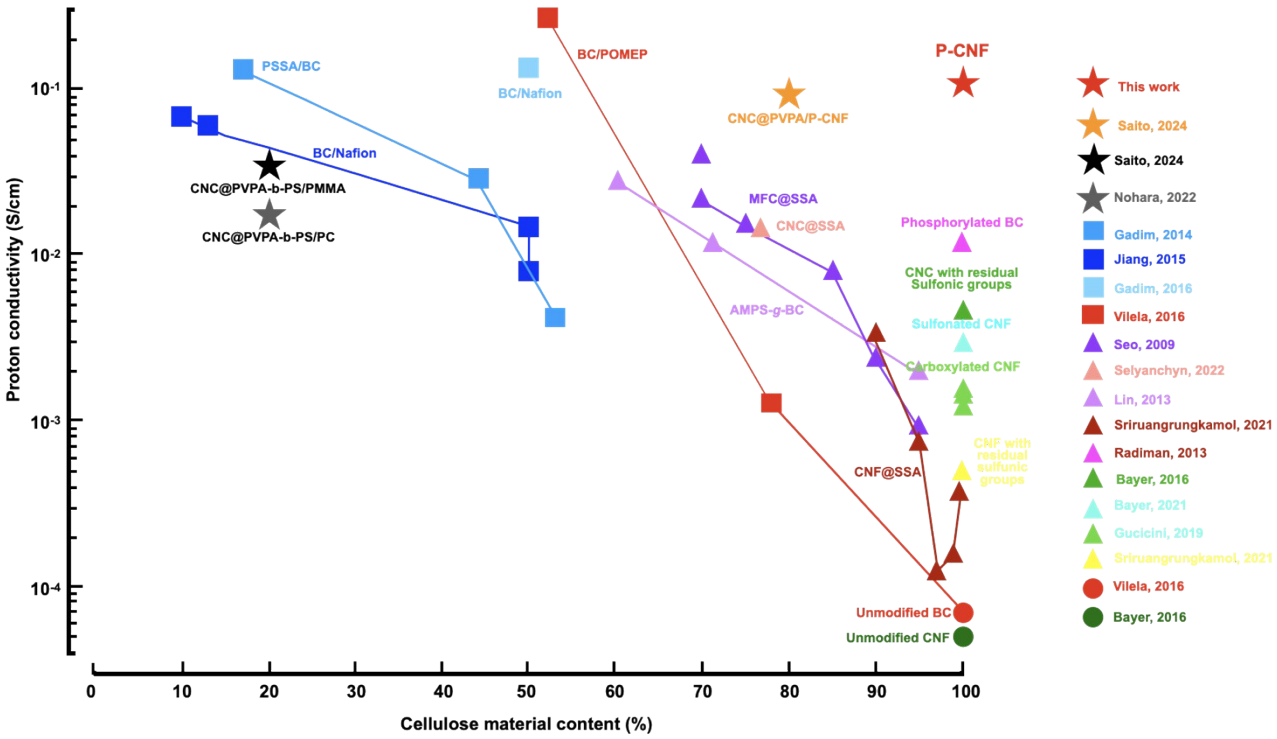

Figure S15. A summary of the proton conductivity in different cellulose composite PEMs, as reported in the literature, depicts the proton conductivity according to the cellulose content in the membranes. The data points marked with stars represent the cellulose composite membranes that we have reported, including this paper. Pure cellulose was represented by circular data points, polymer blends by square data points, and modified cellulose by triangular data points.

Table S5. Comparison of cellulose based PEMs and their performance. (corresponding to Figure 4.)

Membranes	Temp. (°C)	Hmd. (% RH)	Proton conductivity (S/cm)	Ref.
P-CNF (-2 h)	80	95	1.2×10^{-1}	This work
CNC@PVPA/P-CNF	80	95	9.2×10^{-2}	(1)
CNC@PVPA-b-PS /PMMA	80	95	3.1×10^{-2}	(2)
CNC@PVPA-b-PS /PC	60	95	1.8×10^{-2}	(3)
PSSA/BC	94	98	1.3×10^{-1}	(4)
BC/Nafion	30	100	7.1×10^{-2}	(5)
BC/Nafion	94	98	1.4×10^{-1}	(6)
BC/POMEP	80	98	5.5×10^{-1}	(7)
MFC@SSA	25	In water	4.0×10^{-2}	(8)
CNC@SSA	120	96	1.5×10^{-2}	(9)
AMPS-g-BC	R.T.	In water	2.9×10^{-2}	(10)
CNF@SSA	R.T.	In water	3.2×10^{-2}	(11)
Phosphorylated BC	80	100	1.1×10^{-2}	(12)
CNC with residual sulfonic groups	120	100	4.6×10^{-3}	(13)
Sulfonated CNF	120	100	3.0×10^{-3}	(14)
Carboxylated CNF	30	95	1.7×10^{-3}	(15)
CNF with residual sulfunic groups	R.T.	In water	5.0×10^{-3}	(11)
Unmodified BC	80	98	6.0×10^{-5}	(7)
Unmodified CNF	100	100	5.0×10^{-3}	(13)

Table S6. Target values and/or guidelines for the properties required of PEMs, along with a comparison of the performance of Nafion 212, 115, 117, and P-CNF-2h membrane.

Required properties for PEMs	Target values and/or gide line	Nafion 212 [a]	Nafion 115	Nafion 117	P-CNF-2h [a]
Proton conductivity	1.2×10^{-1} S/cm (80°C, 80% RH) (16)	2.1×10^{-1} S/cm (80°C, 95% RH) 6.6×10^{-2} S/cm (20°C, 95% RH)	$5.3 - 7.0 \times 10^{-2}$ S/cm (17)	$7.0 - 9.0 \times 10^{-2}$ S/cm (17)	1.2×10^{-1} S/cm (80°C, 95% RH) 7.1×10^{-2} S/cm (20°C, 95% RH)
IEC	The amount of protons that can be retained and adsorbed by the acidic groups of the PEM through ion-exchange reactions.	0.95 meq/g	0.91 meq/g (18)	0.90 meq/g (19)	3.40 meq/g
Water uptake	Absorption rate of water molecules for proton conduction.	14.6 % (80°C, 95% RH)	-	-	35.0 % (80°C, 95% RH)
Swelling ratio	Dimensional stability with humidification-drying cycles during operating PEFCs.	16.0 % (80°C, 95% RH)	-	-	78.0 % (80°C, 95% RH)
Environmental impact	PFAS-free : Regulation of PFAS	Fluoropolymers	Fluoropolymers	Fluoropolymers	Natural resource, PFAS-free
pKa	Weakly acidic membrane eliminates the need for acid-resistant peripheral components.	-6.0	-6.0	-6.0	$pKa_1 \approx 2.2$, $pKa_2 \approx 7.0$
Tensile test	Prevents PEM damage from mechanical stress applied during cell assembly.	26.1 MPa (Ambient condition)	27.46 MPa (20) (23 °C)	25 MPa (21) (Ambient condition)	111.1 MPa (Ambient condition)
Gas (Oxgen) permeability	The low oxygen permeability is important because oxygen permeation through the PEM causes membrane degradation by radical formation.	3.00×10^3 cm³/(m² · 24h · atm) [c] (40°C, without humidity control)	-	-	2.19 cm³/ (m² · 24h · atm) [c] (40°C, without humidity control)
Thickness	< 8 μm (16)	50 μm	125 μm (22)	175 μm (22)	30-45 μm
Cost	17.5 $/m² (2025 target) (23)	2200 $/m² (17)	2700 $/m² (17)	3200 $/m² (17)	312 $/m² [b]

a Obtained results from this study and our previous study.
b Estimated cost of materials used to synthesize P-CNF.

References

(1) T. Saito, Y. Matsuo, K. Tabata, T. Makino, T. Nohara and A. Masuhara, *Energy Fuels*, 2024, **38**, 4645-4652.

(2) T. Nohara, T. Arita, K. Tabata, T. Saito, R. Shimada, H. Nakazaki, Y. Suzuki, R. Sato and A. Masuhara, *ACS Appl. Mater. Interfaces*, 2022, **14**, 8353-8360.

(3) T. Saito, T. Nohara, K. Tabata, H. Nakazaki, T. Makino, Y. Matsuo, K. Sato, C. Abadie and A. Masuhara, *Energy Fuels*, 2022, **36**, 13924-13929.

(4) T. D. O. Gadim, A. G. P. R. Figueiredo, N. C. Rosero-Navarro, C. Vilela, J. A. F. Gamelas, A. Barros-Timmons, C. P. Neto, A. J. D. Silvestre, C. S. R. Freire and F. M. L. Figueiredo, *ACS Appl. Mater. Interfaces*, 2014, **6**, 7864-7875.

(5) G.-p. Jiang, J. Zhang, J.-l. Qiao, Y.-m. Jiang, H. Zarrin, Z. Chen and F. Hong, *J. Power Sources*, 2015, **273**, 697-706.

(6) T. D. O. Gadim, C. Vilela, F. J. A. Loureiro, A. J. D. Silvestre, C. S. R. Freire and F. M. L. Figueiredo, *Ind. Crops Prod.*, 2016, **93**, 212-218.

(7) C. Vilela, T. D. O. Gadim, A. J. D. Silvestre, C. S. R. Freire and F. M. L. Figueiredo, *Cellulose (Dordrecht, Neth.)*, 2016, **23**, 3677-3689.

(8) J. A. Seo, J. C. Kim, J. K. Koh, S. H. Ahn and J. H. Kim, *Ionics*, 2009, **15**, 555-560.

(9) O. Selyanchyn, T. Bayer, D. Klotz, R. Selyanchyn, K. Sasaki and S. M. Lyth, *Membranes (Basel, Switz.)*, 2022, **12**, 658.

(10) C. W. Lin, S. S. Liang, S. W. Chen and J. T. Lai, *J. Power Sources*, 2013, **232**, 297-305.

(11) A. Sriruangrungkamol and W. Chonkaew, *Polym. Bull. (Heidelberg, Ger.)*, 2021, **78**, 3705-3728.

(12) C. L. Radiman and A. Rifathin, *J. Appl. Polym. Sci.*, 2013, **130**, 399-405.

(13) T. Bayer, B. V. Cunning, R. Selyanchyn, M. Nishihara, S. Fujikawa, K. Sasaki and S. M. Lyth, *Chem. Mater.*, 2016, **28**, 4805-4814.

(14) T. Bayer, B. V. Cunning, B. Smid, R. Selyanchyn, S. Fujikawa, K. Sasaki and S. M. Lyth, *Cellulose. (Dordrecht, Neth.)*, 2021, **28**, 1355-1367.

(15) V. Guccini, A. Carlson, S. Yu, G. Lindbergh, R. W. Lindstroem and G. Salazar-Alvarez, *J. Mater. Chem. A*, 2019, **7**, 25032-25039.

(16) Japan Government, NEDO hydrogen roadmap (in Japanese), 2023, https://www.nedo.go.jp/library/battery_hydrogen.html

(17) M. R. Asghar and Q. Xu, *Journal of Polymer Research*, 2024, **31**, 125.

(18) P. Costamagna, C. Yang, A. B. Bocarsly and S. Srinivasan, *Electrochimica acta*, 2002, **47**, 1023-1033.

(19) B. Ghanti, R. Kamble, H. Komber, B. Voit and S. Banerjee, *Journal of Power Sources*, 2025, **631**, 236201.

(20) C. Ceballos-Alvarez, M. Jafari, M. Siaj, S. Shahgaldi and R. Izquierdo, *Nanomaterials*, 2025, **15**, 68.

(21) M. Gouda, W. Gouveia, N. Elessawy, B. Šljukić, A. A. Nassr and D. Santos, *International Journal of Hydrogen Energy*, 2020, **45**, 15226-15238.

(22) X. Du, J. Yu, B. Yi, M. Han and K. Bi, *Physical Chemistry Chemical Physics*, 2001, **3**, 3175-3179.

(23) Fuel cell Technical Team Roadmap, 2017, www.energy.gov/eere/vehicles/downloads/us-drive-fuel-cell-technical-team-roadmap.